GENERALIZED DESIGN OF MULTI-RESONANT DIPOLE ANTENNAS USING KOCH CURVES

K.J. Vinoy, Jose K. Abraham, and V.K. Varadan
Center for the Engineering of Electronic and Acoustic Materials and Devices
The Pennsylvania State University, 212 EES Building, University Park, PA 16802

Abstract: Generalizations of fractal Koch curves and their use in designing multi-resonant antennas are presented in this paper. Both recursive and non-recursive generalizations of the curve are examined. Variation of the indentation angle is used for this approach. Although this variation has a direct bearing on the unfolded length of the curve, this should be considered as a primary variable since several geometries with the same unfolded length can be constructed with different permutations of indentation angles. Antenna input characteristics such as the primary resonant frequency, the input resistance at this resonance, and ratios of the first few resonant frequencies have been studied by numerical simulations. This study shows that it is possible to design multi-resonant antennas using Koch curves with various indentation angles. Identifying similar parameters with other known fractal geometries would offer a viable route for designing multiband and multifunctional antennas for modern wireless applications using them.

Keywords: Fractals, Multifrequency antennas, Wire antennas.

1. INTRODUCTION

Fractal geometries have found numerous applications in several fields of science and engineering in the past few decades, ever since the term fractal was coined by Mandelbrott for a class of seemingly irregular geometries [1]-[5]. Disciplines such as geology, atmospheric sciences, forest sciences, physiology have all benefited significantly by fractal modeling of several naturally occurring phenomena. In electromagnetics, fractal geometries have been studied in the context of various wave propagation scenarios. Scattering and diffraction from fractal screens have been studied extensively [6]-[7]. More recently fractal geometries have also been used in frequency selective screens [8]-[10]. Similarly, fractal concepts have also been used in antenna engineering. The primary motivation for the use of fractals in this area has been to extend antenna design and synthesis concepts beyond Euclidean geometry [11]-[12]. Obtaining special antenna characteristics using a fractal distribution of elements is the main objective of the study on fractal antenna arrays. Self-similar arrays have frequency independent multi-band characteristics [13].

Antenna elements with fractal shapes have also been investigated in recent years. It is the irregular nature of these geometries that has caught the attention of antenna designers - primarily as a past-time. Over the past decade or so, several antenna properties have been qualitatively linked to the nature of these geometries. With the deepening of such an understanding of relationships between geometric properties and antenna features, a new class of antennas, called fractal shaped antennas is becoming popular. Initial investigations with fractal geometries for antenna applications have been experimental. Fractal geometries such as Koch curves, Minkowski curves, Sierpinski carpets were investigated by Cohen for various types of antennas [14]. Fractal trees were also explored and found to have multiband characteristics [15]. Self-similarity of these fractal geometries has since been qualitatively associated with multiband characteristics of antennas using them. Several self-similar geometries have therefore been explored to obtain multiband antenna characteristics [16]-[19]. For example, Sierpinski gaskets have been studied extensively for monopole and dipole antenna configurations [20]. The self-similar current distribution on these antennas is expected to cause its multi-band characteristics [21]. Yet another fractal geometry pursued by many antenna researchers is the Koch curve. Several variants of this geometry have been used as dipole, monopole, loop and patch antennas with equally diverse performance [14], [22]-[28]. Historically, Koch monopoles are among the first antennas based on a fractal geometry designed as small sized antennas. In addition to being small,

these geometries can potentially lead to multiband antenna characteristics [22].

Fractal shaped antennas for numerous wireless applications have been commercialized recently. The advantages of using fractal shaped antenna elements are manifold. These geometries can lead to antennas with multiband characteristics, often with similar radiation characteristics in these bands. However, it may be pointed out that the ordered nature of fractals introduces a substantial advantage over an antenna geometry obtained by arbitrarily shrinking the geometry, and this could be exploited in novel antenna design and analysis approaches. However, thus far the research on using these geometries, has more or less concentrated on introducing them into the realm of antenna design, without seriously getting into novel design ideas. There are few exceptions including the works by Werner et. al. [28]-[29] where antenna properties were optimized by modifying the geometry using a genetic algorithm. The present authors have reported a design approach for Hilbert curve and Koch cure dipole antennas making use of its fractal features [30]-[33].

In this paper however, it is attempted to make a parametric study of dipole antennas using Koch curves, with the indentation angle as the design parameter. If this angle is kept a constant for various iterations, the resultant geometry is self-similar. A variation in the indentation angle of these self-similar geometries can be used to obtain a parametric correlation between the antenna characteristics and a mathematically expressible feature (e.g., fractal dimension) of the fractal geometry [32]-[33]. However a convenient means for designing such antennas can be obtained if the indentation angles for all iterations are chosen independently. The resultant geometry is non-recursive and may not be truly called fractal.

The geometries studied here may be considered as a special case of those presented in [28] and [29], since the initiator in the present case has one line segment less. The approach for generalization of the geometry is described in the next section. Results of numerical simulations using NEC for antennas with these geometries are described in Section 3. It has been found that the indentation angle of each Koch iteration may be varied to design multi-resonant antennas with variable frequency intervals. A brief summary of the new findings in this paper are presented in Section 4. It is expected that the use of these ideas would significantly reduce the computational intensity of optimization approaches for design of antennas using fractal geometries, and would help antenna designers approach the problem with due merit.

2. GENERALIZATION OF KOCH CURVES

The antenna geometry used in this paper is based on a fractal curve originally introduced by Swedish mathematician Helge von Koch in 1904 [34]. Several generalizations of the original geometry exist. The recursive construction of the basic fractal curve is shown in Fig. 1. To distinguish this from generalizations introduced later, this geometry will be referred to as the *standard Koch curve* for the rest of the discussions.

The geometric construction of the standard Koch curve is fairly simple. One starts with a straight line, called the initiator. This is partitioned into three equal parts, and the segment at the middle is replaced with two others of the same length. This is the first iterated version of the geometry and is called the generator. The process is reused in the generation of higher iterations.

It may be recalled that each segment in the first iterated curve is $^1/_3$ the length of the initiator. There are four such segments. Thus for n^{th} iterated curve the unfolded (or stretched out) length of the curve is $(^4/_3)^n$. This is an important property useful in the design of antennas using them.

2.1. IFS for the Standard Koch Curve

An iterative function system (IFS) can be effectively used to generate the standard Koch curve. A set of affine transformations forms the IFS for its generation. Let us suppose that the initiator (unit length) is placed along the x-axis, with its left end at the origin. The transformations to obtain the segments of the generator are

$$W_1\begin{pmatrix} x' \\ y' \end{pmatrix} = \begin{bmatrix} \frac{1}{3} & 0 \\ 0 & \frac{1}{3} \end{bmatrix}\begin{pmatrix} x \\ y \end{pmatrix}, \tag{1}$$

$$W_2\begin{pmatrix} x' \\ y' \end{pmatrix} = \begin{bmatrix} \frac{1}{3}\cos 60^\circ & -\frac{1}{3}\sin 60^\circ \\ \frac{1}{3}\sin 60^\circ & \frac{1}{3}\cos 60^\circ \end{bmatrix}\begin{pmatrix} x \\ y \end{pmatrix} + \begin{pmatrix} \frac{1}{3} \\ 0 \end{pmatrix}, \tag{2}$$

$$W_3\begin{pmatrix} x' \\ y' \end{pmatrix} = \begin{bmatrix} \frac{1}{3}\cos 60^\circ & \frac{1}{3}\sin 60^\circ \\ -\frac{1}{3}\sin 60^\circ & \frac{1}{3}\cos 60^\circ \end{bmatrix}\begin{pmatrix} x \\ y \end{pmatrix} + \begin{pmatrix} \frac{1}{2} \\ \frac{1}{2}\sin 60^\circ \end{pmatrix}, \tag{3}$$

$$W_4\begin{pmatrix} x' \\ y' \end{pmatrix} = \begin{bmatrix} \frac{1}{3} & 0 \\ 0 & \frac{1}{3} \end{bmatrix}\begin{pmatrix} x \\ y \end{pmatrix} + \begin{pmatrix} \frac{2}{3} \\ 0 \end{pmatrix}. \quad (4)$$

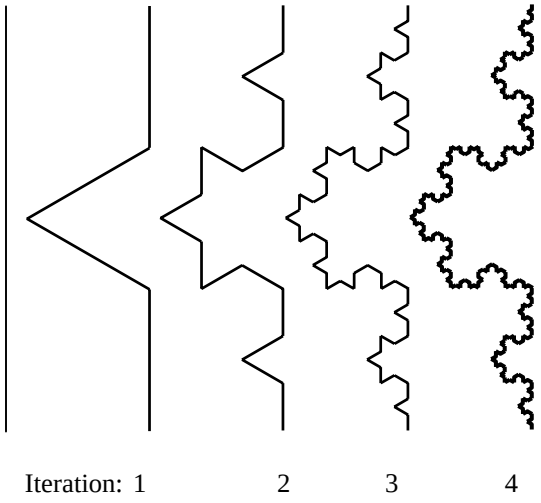

Fig. 1. Geometrical construction of standard Koch curve (indentation angle=60°).

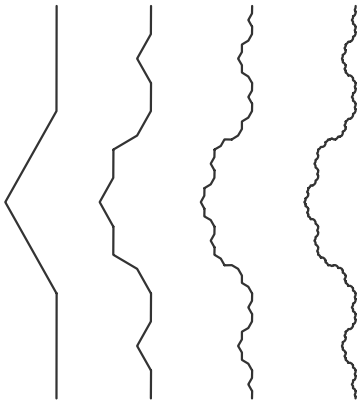

Fig. 2. A recursive generalization based on fractal Koch curves of first four iterations with an identical indentation angle of 30° for various stages.

The generator is then obtained as

$$A_1 = W(A) = W_1(A) \cup W_2(A) \cup W_3(A) \cup W_4(A). \quad (5)$$

This process can be repeated for all higher iterations of the geometry. It may be observed that the (straight line) distance between the start and end points of curves of all iterations is the same. Various iterations of the geometry obtained with this IFS are shown in Fig. 1.

2.2. Recursive Generalizations

In the proposed generalizations studied as part of this work, the rotation (indentation) angle is made a variable. This leads to generalization of IFS with the following transformations

$$W_1\begin{pmatrix} x' \\ y' \end{pmatrix} = \begin{bmatrix} \frac{1}{s} & 0 \\ 0 & \frac{1}{s} \end{bmatrix}\begin{pmatrix} x \\ y \end{pmatrix}, \quad (6)$$

$$W_2\begin{pmatrix} x' \\ y' \end{pmatrix} = \begin{bmatrix} \frac{1}{s}\cos\theta & -\frac{1}{s}\sin\theta \\ \frac{1}{s}\sin\theta & \frac{1}{s}\cos\theta \end{bmatrix}\begin{pmatrix} x \\ y \end{pmatrix} + \begin{pmatrix} \frac{1}{s} \\ 0 \end{pmatrix}, \quad (7)$$

$$W_3\begin{pmatrix} x' \\ y' \end{pmatrix} = \begin{bmatrix} \frac{1}{s}\cos\theta & \frac{1}{s}\sin\theta \\ -\frac{1}{s}\sin\theta & \frac{1}{s}\cos\theta \end{bmatrix}\begin{pmatrix} x \\ y \end{pmatrix} + \begin{pmatrix} \frac{1}{2} \\ \frac{1}{s}\sin\theta \end{pmatrix}, \quad (8)$$

$$W_4\begin{pmatrix} x' \\ y' \end{pmatrix} = \begin{bmatrix} \frac{1}{s} & 0 \\ 0 & \frac{1}{s} \end{bmatrix}\begin{pmatrix} x \\ y \end{pmatrix} + \begin{pmatrix} \frac{s-1}{s} \\ 0 \end{pmatrix}, \quad (9)$$

where the scale factor s is angle dependent and is given by

$$\frac{1}{s} = \frac{1}{2(1+\cos\theta)}. \quad (10)$$

This ensures the distance between the start and end points for all iterations is the same. It may be easily verified that this formulation degenerates to the standard Koch curve for θ=60°.

The generator for the geometry can be obtained as in eq. (5). These affine transformations in the generalized case also lead to a self-similar fractal geometry. As an example, self-similar geometries of various iterations obtained by recursively applying the above transformations have been shown in Fig. 2. The indentation angle in these cases is 30°, as compared to 60° used for the standard Koch curve geometry. In fact this variation in indentation angle causes a corresponding variation in the fractal dimension of the geometry. The fractal similarity dimension of this generalization of the geometry is obtained as

$$D = \frac{\log 4}{\log\left[2(1+\cos\theta)\right]}. \quad (11)$$

Similar geometries with varying fractal similarity dimensions can be obtained for different indentation angles with this recursive generalization. The indentation angle may vary between 0 and 90°. For the indentation angle θ=0, the curve is linear (dimension=1) while for θ=90°, a geometry of sufficiently large iteration tends to fill a triangular area (dimension=2).

2.3. Non-recursive Generalizations

The indentation angle and the scale factor for all stages of iteration are kept the same in the recursive generalization described above. Further generalized curves can be obtained by removing this restriction and are used in the study presented in this paper. In order to ensure that the approach is systematic, all sub-sections of the curve are kept identical. Thus all line segments of the final geometry have the same length, and indentation angles for subsections of the geometry at individual iteration are identical. Such generalizations of a third iterated Koch curve are shown in Fig. 3. The indentation angle for iteration stages are 20°, 40°, and 60°, with the last angle used in the outermost generator for case (c) and vice versa for case (d). For a given end-to-end distance l, the length of individual line segments m constituting an n^{th} iterated geometry is given by

$$m = \frac{l}{2^n \prod_{i=1}^{n} \left(1 + \cos\theta_i\right)}. \tag{12}$$

Likewise, the total unfolded length of the curve is given by

$$L = \frac{2^n l}{\prod_{i=1}^{n} \left(1 + \cos\theta_i\right)}. \tag{13}$$

It may be observed that for a given l, various permutations of angles can result in the same unfolded length. Thus this generalization offers a possibility of studying the effects of indentation angles, as opposed to unfolded length.

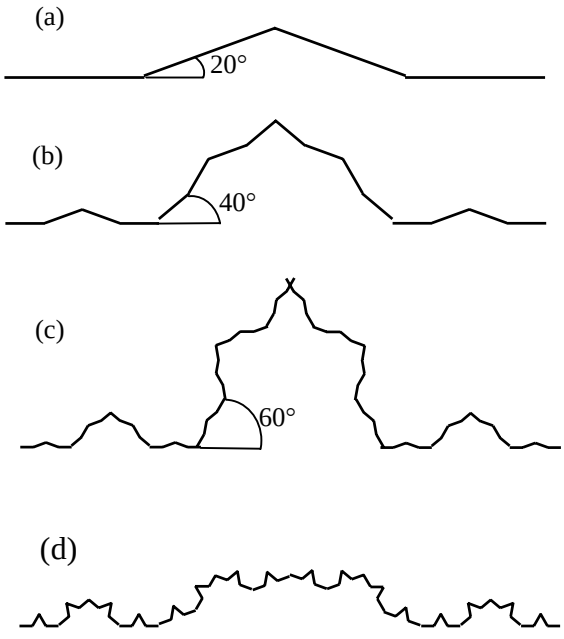

Fig. 3. Generalized curves obtained by non-recursive approach. The curve in (b) has four copies of the one in (a), but with a different indentation angle. Similarly the curves in (c) is obtained from (b). Two such 3rd iterated curvs are compared in (c) and (d). Indentation angles are: (c) 20°-40°-60° (d) 60°-40°-20°. The angle for the first generator listed first.

3. MODELING STUDIES ON THE ANTENNA

3.1. Dipole Antenna Model

Dipole antennas with arms consisting of Koch curves of different indentation angles and fractal iterations are simulated using a moment method based software G-NEC. A typical dipole antenna using 4th order iteration curves with an indentation angle of 60° and with the feed located at the center of the geometry is shown in Fig. 4. Similar geometries with various fractal iterations and indentation angles have been extensively studied by numerical simulations [33]. This model consists of wire elements only. The radius of wire segments constituting the antenna model is consistently kept at 0.1 mm. It may be noted that this values is much smaller than the wavelength (~60 mm) at the highest frequency considered in the present study. The segmentation length used in the NEC model is taken as approximately 0.5 mm, uniform in all cases. Each dipole arm has an end-to-end distance of 10 cm.

3.2. Numerical Simulations of Antennas with Self-Similar Geometry

Characteristics of antennas using the standard Koch curve of this type have been studied previously by experiments as well as numerical

Table 1. Primary (first) resonant frequencies for dipole antennas with self-similar Koch curves (with recursive IFS) for various iterations obtained by numerical simulations. The end-to-end distance of these arms are kept constant at 0.1 m.

Indentation Angle (Deg.)	Unfolded arm length (m) for various iterations				Resonant frequencies (MHz) for various iterations			
	1	2	3	4	1	2	3	4
10	0.101	0.102	0.102	0.103	710.1	713.5	711.7	710.1
20	0.103	0.106	0.116	0.113	685.8	693.9	687.8	685.8
30	0.107	0.115	0.123	0.132	643.2	662.4	649.6	643.2
40	0.113	0.128	0.145	0.164	589.1	618.8	595.1	589.1
50	0.122	0.148	0.18	0.22	512.5	565.6	528.6	512.5
60	0.133	0.178	0.237	0.316	427.9	505.1	453.8	427.9
70	0.149	0.222	0.331	0.493	337.2	441.2	376	337.2
80	0.170	0.290	0.495	0.843	256.6	381.3	304.6	256.6

simulations [22]-[27]. Since these antennas are small in terms of operational wavelength, their radiation performance is not expected to change significantly. Hence only the input characteristics of these antennas are examined in the following discussions.

Resonant frequencies for antennas with various iterations of self-similar geometry have been listed in Table 1. This indicates that by changing the indentation angle or fractal iteration, the resonant frequency can be reduced. However this reduction

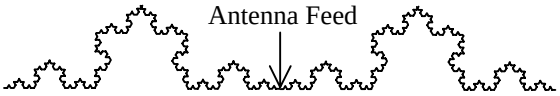

Fig. 4. Configuration of Koch dipole antenna. Arms of the antenna have 4th iteration Koch curves with indentation angle=60°.

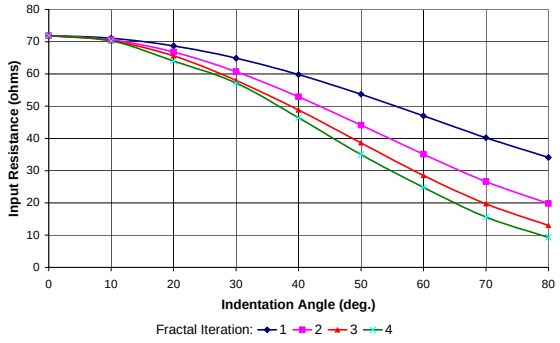

Fig. 5. Variation of input resistance of the dipole antennas with generalized Koch curves (self-similar) of various fractal iterations.

in resonant frequency may as well be attributed to the increase in the unfolded length of the curve. In contrast to previous designs using a genetic algorithm [28]-[29], the present approach strives to generate a knowledge base using geometrical features and hence is expected to be less computation intensive.

The input resistance at the resonant frequency also changes by these modifications to the standard geometry. In Fig. 5, these variations are plotted for various iterations of the fractal. For angle $\theta=0$, these antennas all degenerate to identical linear dipoles with a resonant input resistance of about 72Ω. As the angle or the fractal iteration is increased, this value is reduced significantly. It may be observed that it is always preferable to match the antenna impedance to a standard value (50Ω). Although not attempted in this paper, this approach of generalization may be used to design antennas with the required input characteristics at a specified frequency. In other words, the indentation angle may be used as a design parameter.

The antenna input characteristics at higher resonant frequencies are also altered by the change in angles. To compare these, the variations of first four resonant frequencies are plotted in Fig. 6 for the first four iterations of the geometry. It may be noticed that for very small indentation angles, these antennas behave similar to linear dipoles. However as the angle is increased, the periodicity of these multiple resonances is changed. It may be argued that the indentation angle of the self-similar antenna can be changed for appropriate positioning of its resonant frequencies.

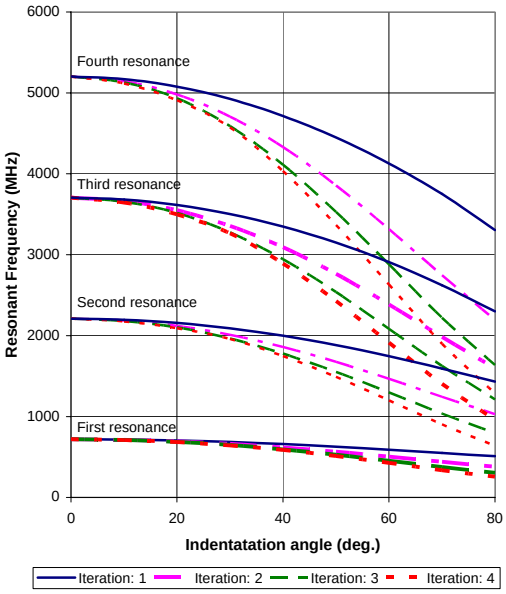

Fig. 6. Variation of resonant frequencies of dipole antennas with generalized self-similar Koch curves of various fractal iterations. The resonant frequencies for each resonance of all cases converge to that of linear dipole when the indentation angle approaches zero.

3.3. Numerical Simulations of Antennas with Non-Recursive Geometry

The geometries used thus far were all generated recursively by using an IFS. If one were to break this rule, antenna properties may be tailored with better flexibility. Although the resulting antenna structure may not be called truly fractal, this offers the possibility of studying curves with the same unfolded length, but with different sets of angles for various iterations. Extensive numerical simulation studies have been performed on antennas using such non-recursive geometries to explore the usefulness of indentation angle, contrary to the unfolded length, as the primary parameter. A few representative cases are presented here.

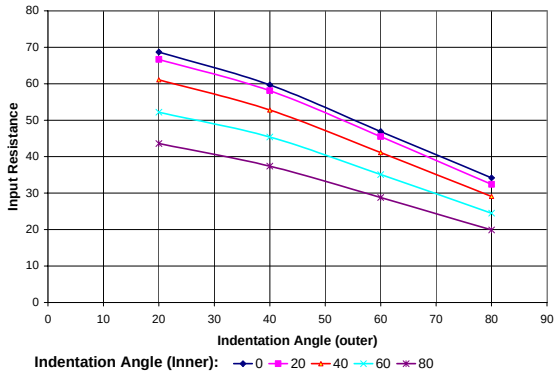

Fig. 7. Input resistance at the first (primary) resonance of dipole antennas based on generalized Koch curves. In all antennas, end-to-end distance of their arms are kept constant at 0.1 m, and have 2nd generation non-recursive Koch curve. The angle at the inner iteration is the parametric variation while the x-axis is for the angle of the outer stage.

In Table 2 the unfolded length of arms of the dipole and the resulting primary resonant frequency are listed. As mentioned earlier, permutations of indentation angles, such as (20°, 40°) and (40°, 20°) lead to the same unfolded length, but different resonant frequencies. This shows that having identical unfolded length does not guarantee similar input characteristics of the antenna. Furthermore a consistent variation in the input resistance of the antenna at its primary resonance is also observed. These are plotted for various indentation angles in Fig. 7. Similarly, the variation in the periodicity of distribution of first four resonant frequencies of various antenna geometries can be observed from Table 3. Thus if one has the flexibility of arbitrarily choosing the indentation angle at each stage of generation of the

Table 2. Unfolded curve length and resonant frequencies for various indentation angles of the non-recursive generalization of the 2nd iterated Koch curve. The end-to-end distance of its arms are kept constant at 0.1 m.

Indentation angle (inner)	Unfolded Curve-Length (m) for various (outer) Indentation angles				Resonant Frequencies (MHz) for (outer) Indentation angles			
	20°	40°	60°	80°	20°	40°	60°	80°
20°	0.106	0.117	0.137	0.176	694	662	610	554
40°	0.117	0.128	0.151	0.193	650	619	570	515
60°	0.137	0.151	0.178	0.227	580	550	505	455
80°	0.176	0.193	0.227	0.290	497	469	427	382

Table 3. Resonant frequencies of dipole antennas with 2nd generation generalized non-recursive Koch curves. The indentation angle in each generation stage is different. The end-to-end distance of these arms are kept constant at 0.1 m.

Indentation Angles		Input Resistance	Resonant Frequencies (MHz)				Ratios of Resonant Frequencies		
Inner	Outer	at f_{r1}	f_{r1}	f_{r2}	f_{r3}	f_{r4}	f_{r2}/f_{r1}	f_{r3}/f_{r2}	f_{r4}/f_{r3}
0	20	68.7	705	2157	3615	5078	3.060	1.676	1.405
	40	59.7	660	1999	3348	4716	3.029	1.675	1.409
	60	46.9	590	1748	2910	4130	2.963	1.665	1.419
	80	34.2	511	1432	2300	3311	2.802	1.606	1.440
20	20	66.7	694	2121	3549	4981	3.056	1.673	1.403
	40	58.1	650	1964	3284	4621	3.022	1.672	1.407
	60	45.5	580	1714	2847	4035	2.955	1.661	1.417
	80	32.4	497	1395	2247	3236	2.807	1.611	1.440
40	20	61.1	662	2012	3354	4690	3.039	1.667	1.398
	40	52.8	619	1861	3093	4332	3.006	1.662	1.401
	60	41.1	550	1619	2666	3748	2.944	1.647	1.406
	80	29.1	469	1308	2093	2991	2.789	1.600	1.429
60	20	52.2	610	1839	3043	4221	3.015	1.655	1.387
	40	45.4	570	1696	2792	3870	2.975	1.646	1.386
	60	35.1	505	1468	2386	3317	2.907	1.625	1.390
	80	24.5	427	1177	1858	2619	2.756	1.579	1.410
80	20	43.6	554	1648	2689	3663	2.975	1.632	1.362
	40	37.4	515	1513	2451	3336	2.938	1.620	1.361
	60	28.8	455	1299	2075	2828	2.855	1.597	1.363
	80	19.9	382	1031	1599	2194	2.699	1.551	1.372

curve, antennas with varied input characteristics can be obtained.

Similar variations in input characteristics are also obtained for antennas with 3rd iteration geometries. Resonant frequencies of antenna geometries with various permutations of indentation angles, with the innermost angle kept constant at 60° are listed in Table 4.

Following this approach one can have several curves with the same length, but with a different set of resonant frequencies. These differences in resonant frequencies are found to be more pronounced as the order of iteration is increased. Hence this approach offers a scheme of designing antennas based on Koch curves suiting the requirements in terms of both the input resistance and the resonant frequency. It is concluded from this study one can design multi-resonant antennas with considerable flexibility by choosing their indentation angles arbitrarily for each iteration while generating the geometry.

4. CONCLUSIONS

In this paper, the variation in the input characteristics of multi-resonant antennas based on generalizations of fractal Koch curves is presented. Geometries considered here include both recursive and non-recursive curves. Schemes for such generalization of these geometries are introduced. In this study, the indentation angle in the transformations of the iterated function system is varied to obtain a set of geometries. Although this variation has a direct bearing on the unfolded length of the curve, the indentation angle should be considered a primary variable since several geometries with the same unfolded length can be constructed with different permutations of indentation angles. Antenna parameters such as the primary resonant frequency, the input resistance at this resonance, and ratios of the first few resonant frequencies have been studied by numerical simulations. This study shows that it is possible to design multi-resonant antennas using Koch curves by individually choosing an optimum indentation angle for various iteration stages of the

Table 4. Resonant frequencies of 3rd iterated non-recursive geometry. The innermost angle is kept $\theta_1 = 60°$. The other angles are varied as listed.

θ_2	θ_3	Input resistance at f_{r1}	Resonant Frequencies (MHz)				Ratios of Resonant Frequencies		
			f_{r1}	f_{r2}	f_{r3}	f_{r4}	f_{r2}/f_{r1}	f_{r3}/f_{r2}	f_{r4}/f_{r3}
0	20	57.5	649	1968	3281	4589	3.032	1.667	1.399
	40	49.6	605	1815	3017	4223	3.000	1.662	1.400
	60	38.6	537	1571	2582	3632	2.926	1.644	1.407
	80	27.2	456	1261	1995	2848	2.765	1.582	1.428
20	20	55.7	638	1932	3215	4491	3.028	1.664	1.397
	40	48.2	595	1780	2952	4129	2.992	1.658	1.399
	60	37.1	526	1539	2523	3547	2.926	1.639	1.406
	80	25.7	443	1229	1952	2798	2.774	1.588	1.433
40	20	50.4	605	1822	3018	4194	3.012	1.656	1.390
	40	43.4	563	1677	2762	3841	2.979	1.647	1.391
	60	33.3	497	1445	2349	3285	2.907	1.626	1.398
	80	23.1	417	1150	1816	2586	2.758	1.579	1.424
60	20	42.6	553	1646	2697	3709	2.976	1.639	1.375
	40	36.4	513	1509	2457	3380	2.942	1.628	1.376
	60	27.8	451	1294	2077	2870	2.869	1.605	1.382
	80	19	376	1023	1598	2234	2.721	1.562	1.398
80	20	33.7	489	1428	2295	3099	2.920	1.607	1.350
	40	29.1	454	1307	2087	2818	2.879	1.597	1.350
	60	22	397	1113	1753	2369	2.804	1.575	1.351
	80	14.8	328	871	1335	1820	2.655	1.533	1.363

underlying fractal geometry. Identifying similar parameters for other known fractal geometries would ease the complexity in designing multiband and multifunctional antennas for modern wireless applications.

REFERENCES

[1] B.B. Madelbrot, *The Fractal Geometry of Nature*, New York: W.H. Freeman, 1983.

[2] H.-O. Peitgen, J.M. Henriques, L.F. Penedo (Eds.), *Fractals in the Fundamental and Applied Sciences*, Amsterdam: North Holland, 1991.

[3] G.P. Cherepanov, A.S. Balankin, and V.S. Ivanova, "Fractal fracture mechanics," *Engineering Fracture Mechanics*, vol. 51, pp. 997-1033, 1995.

[4] J.H. Jeng, V.V. Varadan, and V.K. Varadan, "Fractal finite element mesh generation for vibration problems," *J. Acous. Soc. Amer.*, vol. 82, pp. 1829-1833, 1987.

[5] A.E. Jacquin, "Fractal image coding: A review," *Proc. IEEE*, vol. 81, pp. 1451-1465, 1993.

[6] A. Lakhtakia, N.S. Holter, V.K. Varadan, and V.V. Varadan, "Self-similarity in diffraction by a self-similar fractal screen," *IEEE Trans. Ant. Propagat.*, vol. 35, pp. 236-239, 1987.

[7] D.L. Jaggard, "Fractal electrodynamics: From super antennas to superlattices," in *Fractals in Engineering*, Springer, pp. 204-221, 1997.

[8] J. Romeu and Y. Rahmat-Samii, "Dual band FSS with fractal elements," *Electron. Lett.*, vol. 35, pp. 702-703, 1999.

[9] D.H. Werner and D. Lee, "Design of dual-polarised multiband frequency selective surfaces using fractal elements," *Electron. Lett.*, vol. 36, pp. 487-488, 2000.

[10] J. Romeu and Y. Rahmat-Samii, "Fractal FSS: a novel dual-band frequency selective surface," *IEEE Trans. Ant. Propagat.*, vol. 48, pp. 1097-1105, 2000.

[11] D.H. Werner, R.L. Haupt, and P.L. Werner, "Fractal antenna engineering: The theory and design of fractal antenna arrays," *IEEE Ant. Propagat. Mag.*, vol. 41, no. 5, pp. 37-59, 1999.

[12] D.H. Werner, P.L. Werner, D.L. Jaggard, A.D. Jaggard, C.Puente, and R.L. Haupt, "The theory and design of fractal antenna arrays," in *Frontiers in Electromagnetics*, D.H. Werner and R. Mittra (Eds.), New York: IEEE Press, pp. 94-203, 1999.

[13] D.H. Werner, P.L. Werner, and A.J. Ferraro, "Frequency independent features of self-similar fractal antennas," IEEE AP-S Inter. Symp. 1996, pp. 2050-2053, 1996.

[14] N. Cohen, "Fractal antenna applications in wireless telecommunications," in Professional Program Proc. of Electronics Industries Forum of New England, 1997, IEEE, pp. 43-49, 1997.

[15] C. Puente, J. Claret, F. Sagues, J. Romeu, M.Q. Lopez-Salvans and R Pous, "Multiband properties of a fractal tree antenna generated by electrochemical deposition," *Electron. Lett.*, vol. 32, pp. 2298-2299, 1996.

[16] C. Puente, J. Romeu, R. Bartoleme, and R. Pous, "Fractal multiband antenna based on Sierpinski gasket," *Electron. Lett.*, vol. 32, pp. 1-2, 1996.

[17] D.H. Werner, A. Rubio Bretones, and B.R. Long, "Radiation characteristics of thin-wire ternary fractal trees," *Electron. Lett.*, vol. 35, pp. 609-610, 1999.

[18] M. Sindou, G. Ablart and C. Sourdois, "Multiband and wideband properties of printed fractal branched antennas," *Electron. Lett.*, vol. 35, pp. 181-182, 1999.

[19] X. Liang and. M.Y.W. Chia, "Multiband characteristics of two fractal antennas," *Microw. Opt. Technol. Lett.*, vol. 23, pp. 242-245, 1999.

[20] C. Puente, M. Navarro, J. Romeu, and R. Pous, "Variations on the fractal Sierpinski antenna flare angle," IEEE AP-S Inter. Symp., pp. 2340-2343, 1998.

[21] M. Navarro, J.M. Gonzalez, C. Puente, J. Romeu, and A. Aguasca, "Self-similar surface current distribution on fractal Sierpinski antenna verified with infra-red thermograms," IEEE AP-S Inter. Symp., pp. 1566-1569, 1999.

[22] C. Puente-Baliarda, J. Romeu, R. Pous, J. Ramis, and A. Hijazo, "Small but long Koch fractal monopole," *Electron. Lett.*, vol. 34, pp. 9-10, 1998.

[23] C.P. Baliarda, J. Romeu, and A. Cardama, "The Koch monopole: A small fractal antenna," *IEEE Trans. Ant. Propagat.*, vol. 48 pp. 1773-1781, 2000.

[24] J.P. Glanvittorio and Y. Rahmaat-Samii, "Fractal element antennas: A compilations of configurations with novel characteristics," IEEE AP-S Inter. Symp. 2000, pp. 1688-1691, 2000.

[25] S.R. Best, "On the resonant behavior of the small Koch fractal monopole antenna," *Microw. Opt. Technol. Lett.*, vol. 35, pp. 311-315, 2002.

[26] S.R. Best, "On the multiband behavior of the Koch fractal monopole antenna," *Microw. Opt. Technol. Lett.*, vol. 35, pp. 371-374, 2002.

[27] S.R. Best, "On the performance of the Koch fractal and other bent wire monopoles as electrically small antennas," IEEE AP-S Inter. Symp. 2002, vol. 4, pp. 534-537, 2002.

[28] D.H. Werner, P.L. Werner and K.H. Church, "Genetically engineered multiband fractal antennas," *Electron. Lett.*, vol. 37, pp. 1150-1151, 2001.

[29] D.H. Werner, P.L. Werner K.H. Church, J.W. Culver, and S.D. Eason, "Genetically engineered dual-band fractal antennas," IEEE AP-S Inter. Symp. 2001, Vol. 3, pp. 628-631, 2001.

[30] K.J. Vinoy, K.A. Jose, V.K. Varadan, and V.V. Varadan, "Resonant frequency of Hilbert curve fractal antennas," in: IEEE AP-S Inter. Symp., vol. 3, pp. 648-651, 2001.

[31] K.J. Vinoy, K.A. Jose, and V.K. Varadan, "On the relationship between fractal dimension and the performance of multi-resonant dipole antennas using Koch curves," *IEEE Trans. Antennas Propagat.* Accepted for publication (Oct 2003).

[32] K.J. Vinoy, K.A. Jose, and V.K. Varadan, "Multiband characteristics and fractal dimension of dipole antennas with Koch curve geometry," IEEE AP-S Inter. Symp., 2002.

[33] K.J. Vinoy, "Fractal shaped antenna elements for wide- and multi-band wireless applications," Ph.D. Dissertation. Pennsylvania State University, 2002.

[34] H.O. Peitgen, H. Jurgens, and D. Saupe, *Chaos and Fractals: New Frontiers of Science*, New York: Springer-Verlag, 1992.

K.J. Vinoy received Bachelors degree from the University of Kerala, India, Masters degree from Cochin University of Science and Technology, India and Ph.D. degree from the Pennsylvania State University in 1990, 1993, and 2002, respectively. From 1994 to1998 he worked in the computational electromagnetics group at National Aerospace Laboratories, Bangalore, India. He was a research assistant at the Center for the Engineering of Electronic and Acoustic Materials and Devices (CEEAMD) at the Pennsylvania State University, from 1999 to 2002. Presently he is continuing there for Post Doctoral research. His research interests include fractal shaped antennas, RF-MEMS, micromachined antennas, and computational electromagnetics. He has published over 30 papers in technical journals and conferences. His publications include two books: *Radar Absorbing Materials: From Theory to Design and Characterization*, (Boston: Kluwer, 1996) and *RF MEMS and their Applications* (London: John Wiley, 2002). He also holds one US patent.

Jose K. Abraham received Ph.D. degree from Cochin University of Science and Technology, India in 1989. From 1990 to 1997 he worked as a Lecturer at Cochin University of Science and Technology, India and was involved with the development of superconducting antennas, radar absorbing materials and wideband microstrip antennas. He joined theCenter for the Engineering of Electronic and Acoustic Materials at Pennsylvania State University in 1997. Currently he is an Assistant Professor of Engineering Science and Mechanics Department. He has published 100 papers in technical Journals and conferences and published a book. He holds two patents. His current research interests include RF MEMS, microwave material characterization, RF wireless sensors and smart antennas.

Vijay K. Varadan received his Ph.D. degree from Northwestern University in 1974. After serving on the faculty of Cornell University and Ohio State University, he joined the Pennsylvania State University in 1983 where he is currently an alumni distinguished professor of engineering science and electrical engineering. He is involved in all aspects of wave-material interaction, optoelectronics, microelectro-nics, microelectromechanical systems (MEMS), smart materials and structures, sonar-, radar-, microwave-, and optically absorbing composite media, FSS, Nanotechnology, Carbon nanotubes, Fuel cells and button cell batteries, EMI shielding materials and piezoelectric, chiral, ferrite, and polymer composites, tunable ceramics materials, and electronically steerable antennas. He is also interested in microwave and ultrasonic experiments to measure the dielectric, magnetic, mechanical and optical properties of composites. He is an Editor of the journal of the Wave-Material Interaction and the Editor-in-Chief of the Journal of Smart Materials and Structures. He has published more than 400 Journal and 300 Proceedings papers and 9 books. He has 10 patents awarded and two pending. He is the Director of the Center for the Engineering of Electronic and Acoustic Materials and Devices. The Center is supported by industries around the world and Government Agencies.